Available online at www.sciencedirect.com

SCIENCE DIRECT®

Journal of Molecular Catalysis A: Chemical 200 (2003) 69–79

JOURNAL OF MOLECULAR CATALYSIS A: CHEMICAL

www.elsevier.com/locate/molcata

o-Alkyl-substituted aromatic phosphanes for hydroformylation studies: synthesis, spectroscopic characterization and ab initio investigations

Helena Riihimäki [a,*], Pekka Suomalainen [b], Heidi K. Reinius [c], Johanna Suutari [c], Sirpa Jääskeläinen [b], A.O.I. Krause [c], Tapani A. Pakkanen [b], Jouni T. Pursiainen [a]

[a] *Department of Chemistry, University of Oulu, P.O. Box 3000, FIN-90014 Oulu, Finland*
[b] *Department of Chemistry, University of Joensuu, P.O. Box 111, FIN-80101 Joensuu, Finland*
[c] *Department of Chemical Technology, Helsinki University of Technology, P.O. Box 6100, FIN-02015 Hut, Finland*

Received 19 September 2002; received in revised form 21 September 2002; accepted 28 October 2002

Abstract

In earlier hydroformylation studies modification of the rhodium catalyst with *o*-methyl-substituted or *o*-ethyl-substituted phosphane ligands have increased regioselectivity to branched aldehydes. The promising results achieved created a need for further studies. Hence, a wider group of *o*-substituted arylphosphane ligands, e.g. (2-cyclohexylphenyl)diphenylphosphane, (2-isopropylphenyl)diphenylphosphane, (2-methylnaphthyl)diphenylphosphane, (2,5-dimethylphenyl)diphenylphosphane and (2-phenylphenyl)diphenylphosphane were synthesized and tested in rhodium-catalyzed hydroformylation to support the previous findings. Characterization of the ligands was made by NMR spectroscopy (^{1}H, ^{31}P{^{1}H}, ^{13}C{^{1}H}, HSQC, COSY-90 and COLOC). Additional parameters for evaluation of the stereoelectronic properties of the ligands were provided by quantum mechanical calculations and by synthesizing Rh(acac)(CO)(PR_3) complexes. In the rhodium-catalyzed hydroformylation of propene and 1-hexene the ligands increased the formation of branched aldehydes compared to triphenylphosphane. Additionally the increasing size of the *o*-alkyl-substituent was found to effect favorably to the *iso*-selectivity.

Keywords: Phosphane ligands; *o*-Alkyl-substituents; Hydroformylation; NMR spectroscopy; Ab initio calculations

1. Introduction

Hydroformylation of propene yielding *n*-butanal and isobutanal is the most important hydroformylation process on industrial scale, providing about 75% of all oxo chemicals consumed in the world [1–4]. Traditionally the aim of this process has been to produce regioselectively the linear aldehyde, *n*-butanal. Recently, interest has increased in selective formation of the branched form, isobutanal, which finds use in the production of polyols, such as neopentyl glycol [4]. This has extended the importance and also the synthetic modification scope of phosphane ligands.

The interest in the steric and electronic properties of phosphanes is based on the assumption that donor/acceptor properties and the bulkiness of the ligand strongly influence the course of the reaction at a transition metal center. Tolman's electronic and

* Corresponding author. Tel.: +358-8-5531647; fax: +358-8-5531603.
E-mail address: helena.riihimaki@oulu.fi (H. Riihimäki).

1381-1169/03/$ – see front matter
doi:10.1016/S1381-1169(03)00022-0

steric parameters (ν and θ, respectively) have formed the basis for the description of steric and electronic properties of phosphanes during the last 30 years [5–7]. High hydroformylation rates of olefins have been found with Rh-catalysts containing bulky *o-tert*-butyl-substituted phenylphosphites with large cone angles (175–180°) [8–11]. As a result from the large cone angles, in $HRh(CO)_n(PR_3)_m$-type catalyst, only one phosphite coordinates to the Rh-center. The sterically hindered phosphite ligands with strongly electron-withdrawing nature (χ-value ∼28) have strong aptitude for CO dissociation compared with the triphenylphosphane (145°, χ-value ∼13), and the formed $16e^-$ complex easily binds to the olefin, thus initiating a very fast reaction cycle. Due to the large space available in comparison with the $HRh(CO)_2(PPh_3)_2$ system, the reaction favor branched aldehyde products, resulting in a moderate overall linearity [8–10]. The same trend to form $16e^-$ complexes has been noticed with bulky nonlinear alkylphosphane-modified catalysts [12]. The high rates of isomerization caused by bulky *o-tert*-butyl-substituted phenylphosphites and thereby the relatively high rates of hydroformylation of internal olefins explain also the high *i*/*n* ratios [10,11]. The improvements in NMR techniques and molecular modeling have given new possibilities to study the properties of phosphane and phosphite ligands [9,13–18]. Today, molecular modeling techniques are more and more used to rationalize structure/reactivity relationships, while ab initio calculations give an insight into the electronic structure of organometallic complexes [18].

Although regioselectivity in the hydroformylation of alkenes depends on a number of factors, one of the most important in the corresponding reaction system are the effects induced by the catalyst. The property of aromatic phosphane ligands in combination with *o*-substituents has been studied mainly with heteroatom containing substituent groups [19–26]. These potential bidentate ligands have proved to be useful in modifying the electronic and steric properties of reactive metal centers. However, the heteroatom modification ($–SCH_3$, $–N(CH_3)_2$, $–OCH_3$ and $–CF_3$) turned out to be unsuccessful in propene hydroformylation decreasing the conversion markedly, and in some cases the hydroformylation reaction was totally hindered.

The preparation and utilization of non-polar *o*-alkyl-substituted phosphanes has been studied only in a few reports [4,21,27–29]. *o*-Methylphenyldiphenylphosphane ligand as a part of $PtCl_2$(cod)/$SnCl_2$ catalyst in the hydroformylation of 2-butene has enhanced selectivity to the branched aldehyde [28]. Moreover, in the hydroformylation of propene, we achieved enhanced selectivity to isobutanal relative to triphenylphosphane through modification of rhodium catalyst with *o*-alkyl-substituted triphenyphosphane [4]. High *i*/*n* ratios were obtained with (*o*-methylphenyl)diphenylphosphane (*o*-MeP), (*o*-ethylphenyl)diphenylphosphane (*o*-EtP) and (2,4,5-trimethylphenyl)diphenylphosphane (2,4,5-MeP), but unfortunately the activities remained low [4].

The promising results containing *o*-methyl-substituted and *o*-ethyl-substituted phenylphosphanes for controlling the product formation upon hydroformylation of propene and 1-hexene achieved created a need for further systematic investigations. Ligands with still bulkier *o*-substituents have now been examined as a modifiers for rhodium catalysts designed for hydroformylation. The present paper describes the preparation and characterization by NMR spectroscopy of (2-cyclohexylphenyl)diphenylphosphane (**1**), (2-isopropylphenyl)diphenylphosphane (**2**), (2-methylnaphthyl)diphenylphosphane (**3**), (2,5-dimethylphenyl)diphenylphosphane (**4**) and (2-phenylphenyl)diphenylphosphane (**5**) ligands (see Scheme 1). The ligands were tested in the hydroformylation of propene and 1-hexene. In spite of the different experimental setups for the two alkenes comparison was considered reasonable because the effects of the different ligands were examined relative to the reaction with PPh_3 modified catalyst. Furthermore, the use of different Rh-species were sought to be justified, as the formation of actual catalyst species, trigonal bipyramidal rhodium carbonyl hydride can be formed from various rhodium precursors.

The crystal structures of *trans*-Rh(CO)Cl(*o*-MeP)$_2$ complex (*o*-MeP = *o*-methylphenyldiphenylphosphane) showed earlier that the *o*-alkyl-substituents were very close to the metal center [29]. The interesting finding concerning the location of *o*-alkyl-substituents inspired to additional studies and so the stereoelectronic effect of the ligands on the hydroformylation reaction was probed by experimental and theoretical methods. $Rh(acac)(CO)(PR_3)$ complexes were prepared and characterized in order to investigate the coordination properties of the ligands. Geometrical

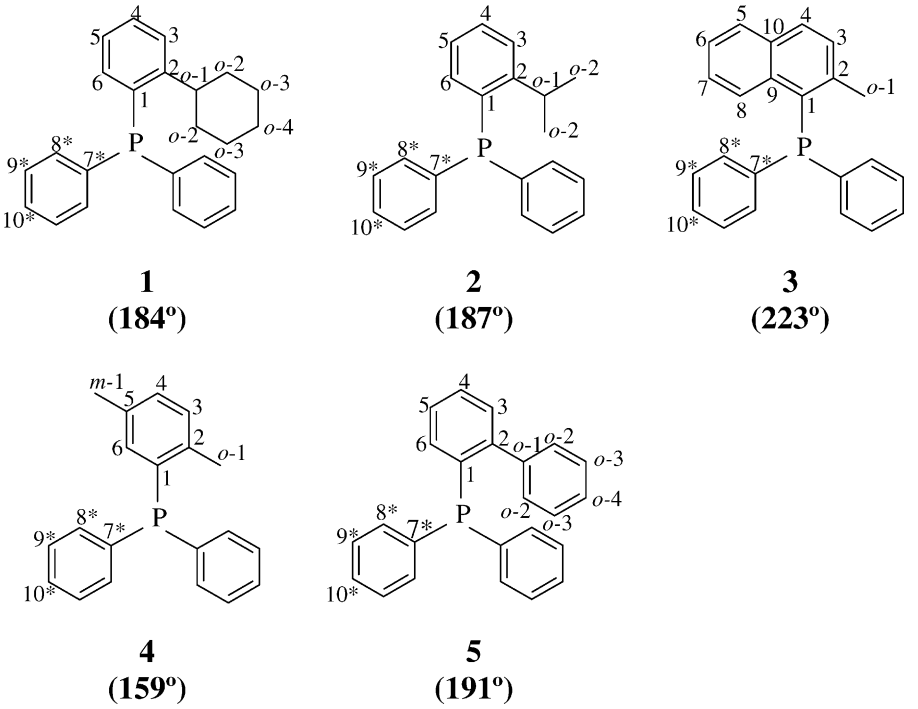

Scheme 1. Schematic structures of the reported ligands (numbering corresponds to the NMR data). Cone angles (°) are given in parentheses.

arrangement and steric size (cone angle) of the free and coordinated ligands were studied theoretically by ab initio Hartree–Fock and DFT methods. Data obtained are discussed in relation to the results of the hydroformylation of propene and 1-hexene.

2. Experimental

General remarks: The used phosphanes are air- and moisture-sensitive, both as pure compounds and in solution, and unprotected show observable oxidation within 1 day. Thus, all reactions were carried out with standard Schlenk techniques under nitrogen or argon atmosphere. The ligands were recrystallized from ethanol or a mixture of ethanol and hexane. 2-Bromotoluene (99%), 1-bromo-2-methylnaphthalene (90%), bromobenzene (99%), 2-bromobiphenyl (96%), chlorodiphenylphosphane (95%), *n*-butyllithium (2.5 M solution in hexane) and (acetylacetonato)dicarbonylrhodium(I) (98%) were obtained from Aldrich. 1-Bromo-2-isopropylbenzene (97%) and 1-bromo-2-cyclohexylbenzene (97%) were from Lancaster and *p*-xylene (99%) was from Fluka. Diethyl ether and tetrahydrofuran were distilled over sodium-benzophenone ketyl under nitrogen before use.

Spectroscopy: The characterization of the ligands was based on ^{1}H-, ^{13}C{^{1}H}-, ^{31}P{^{1}H}-, COSY-90-, HSQC- and COLOC-NMR spectroscopy. NMR spectra were recorded on a Bruker DPX400 spectrometer at room temperature in $CDCl_3$ (99.8% D, 0.03% TMS). NMR spectra of the metal complexes were recorded on a Bruker AM250 spectrometer. ^{1}H-NMR: reference $SiMe_4$. ^{13}C{^{1}H}-NMR: $CDCl_3$ set to 77.0 ppm. ^{31}P{^{1}H}-NMR: external standard 85% H_3PO_4. ^{13}C{^{1}H}- and ^{31}P{^{1}H}-NMR shifts of the free ligands are presented in Tables 1 and 2, respectively. Exact mass peaks for ligands were determined on a Micromass LCT, using ESI+ method.

2.1. Synthesis of ligands

2.1.1. (2-Cyclohexylphenyl)diphenylphosphane (*1*)

A solution of *n*-butyllithium (8.4 ml, 20.9 mmol) was transferred dropwise via a canula to a freshly prepared solution of 1-bromo-2-cyclohexylbenzene

Table 1
$^{13}C\{^1H\}$-NMR spectra (100 MHz, $CDCl_3$) of studied ligands **1**–**5** (see Scheme 1)

	1	**2**	**3**	**4**	**5**
$C^{o\text{-}4}$ (ppm)	26.11	–	–	–	128.66
	(s)	–	–	–	(s)
$C^{o\text{-}3}$ (ppm)	26.77	–	–	–	127.54
	(s)	–	–	–	(s)
$C^{o\text{-}2}$ (ppm)	34.10	23.87	–	–	129.69
$^4J_{CP}$ (Hz)	(s)	(s)	–	–	3.0 (d)
$C^{o\text{-}1}$ (ppm)	41.82	31.24	24.38	20.69	141.68
$^3J_{CP}$ (Hz)	24.3 (d)	24.7 (d)	22.1 (d)	20.8 (d)	6.4 (d)
$C^{m\text{-}1}$ (ppm)	–	–	–	21.05	–
$^4J_{CP}$ (Hz)	–	–	–	(s)	–
C^5 (ppm)	125.86	125.97	128.59	129.96	127.15
	(s)	(s)	(s)	(s)	(s)
C^3 (ppm)	126.07	125.41	129.71	130.02	130.08
$^3J_{CP}$ (Hz)	4.8 (d)	4.7 (d)	5.4 (d)	(s)	4.7 (d)
C^{9*} (ppm)	128.39	128.45	128.41	128.49	128.34
$^3J_{CP}$ (Hz)	6.9 (d)	6.5 (d)	5.6 (d)	7.1 (d)	7.1 (d)
C^{10*} (ppm)	128.55	128.58	127.53	128.71	128.43
	(s)	(s)	(s)	(s)	(s)
C^4 (ppm)	129.02	129.24	131.15	129.53	127.34
$^4J_{CP}$ (Hz)	(s)	(s)	1.4 (d)	(s)	(s)
C^6 (ppm)	133.35	133.35	124.88	133.23	134.08
$^5J_{CP}$ (Hz)	(s)	(s)	1.3 (d)	(s)	(s)
C^{8*} (ppm)	133.95	133.94	131.53	133.97	133.88
$^2J_{CP}$ (Hz)	19.8 (d)	20.4 (d)	18.3 (d)	19.6 (d)	20.0 (d)
C^1 (ppm)	134.84	134.43	136.64	136.12	135.86
$^1J_{CP}$ (Hz)	10.4 (d)	11.1 (d)	10.8 (d)	8.1 (d)	14.4 (d)
C^{7*} (ppm)	137.21	137.21	136.49	135.28	137.64
$^1J_{CP}$ (Hz)	10.4 (d)	11.0 (d)	13.9 (d)	(s)	11.7 (d)
C^2 (ppm)	152.16	153.33	145.67	139.09	148.25
$^2J_{CP}$ (Hz)	23.4 (d)	23.8 (d)	19.1 (d)	24.8 (d)	28.6 (d)
C^7 (ppm)	–	–	125.96	–	–
$^4J_{CP}$ (Hz)	–	–	1.4 (d)	–	–
C^8 (ppm)	–	–	128.15	–	–
$^3J_{CP}$ (Hz)	–	–	19.8 (d)	–	–
C^9 (ppm)	–	–	128.81	–	–
$^2J_{CP}$ (Hz)	–	–	17.4 (d)	–	–
C^{10} (ppm)	–	–	132.84	–	–
$^3J_{CP}$ (Hz)	–	–	3.1 (d)	–	–

Table 2
$^{31}P\{^1H\}$-NMR and FT-IR spectroscopic data of free and coordinated phosphanes

Ligand (PR_3)	Free PR_3	$Rh(acac)(CO)(PR_3)$		
	$^{31}P\{^1H\}$-NMR	$^{31}P\{^1H\}$-NMR		FT-IR
	δ_P (ppm)	δ_P (ppm)	$^1J_{P-Rh}$ (Hz)	υ(CO) (cm^{-1})
1	−13.6	–	–	1977
2	−13.8	44.8	175	1974
3	−16.5	41.4	171	1978
4	−9.5	–	–	1976
5	−11.9	–	–	1975

(5.0 g, 20.9 mmol) in diethyl ether (50 ml) at −10 → 0 °C (salted ice bath). The bright mixture was stirred for 2 h at this temperature, after which a solution of chlorodiphenylphosphane (4.6 g, 3.8 ml, 20.9 mmol) in diethyl ether (30 ml) was added slowly. The addition colored the reaction mixture first light yellow and finally white. Stirring was continued for a further 2 h at −10 → 0 °C. After slow warming to room temperature, some solid material precipitated (inorganic salts). Solid and liquid layers were separated by filtration and solvent was removed in vacuo. The crude yellow and oily product was obtained from the solvent phase and recrystallized from ethanol. The yield of the white pure product was 5.2 g, 15.0 mmol, 72%. Exact mass (Micromass LCT, ESI+): 345.1746 $(M + H)^+$ (calcd. for $C_{24}H_{26}P$, 345.1772). ^{1}H-NMR (400 MHz, $CDCl_3$, see Scheme 1 for numbering) δ_H: 1.15–1.25 (m, 2 H, H^{o-4}), 1.35 (m, 4H, H^{o-2}), 1.60–1.75 (m, 4H, H^{o-3}), 3.29 (m, 1H, H^{o-1}), 6.83 (m, 1H, H^6), 7.06 (m, 1H, H^5), 7.26–7.34 (m, 12H, H^3, H^4, H^{8*}, H^{9*} and H^{10*}). $^{13}C\{^1H\}$- and $^{31}P\{^1H\}$-NMR shifts are presented in Tables 1 and 2.

*2.1.2. (2-Isopropylphenyl)diphenylphosphane (**2**)*

With the procedure described above for (2-cyclohexylphenyl)diphenylphosphane, reactions of 1-bromo-2-isopropylbenzene (6.0 g, 30.0 mmol), *n*-butyllithium (12.0 ml, 30.0 mmol) and chlorodiphenylphosphane (6.6 g, 5.6 ml, 30.0 mmol) afforded a crude oily product. A white solid product was obtained by washing the oily product with hexane/ethanol mixture. The product was recrystallized from ethanol. The yield of the white pure product was 2.1 g, 7.0 mmol, 23%. Exact mass (Micromass LCT, ESI+): 305.1465 $(M + H)^+$ (calcd. for $C_{21}H_{22}P$, 305.1459). ^{1}H-NMR (400 MHz, $CDCl_3$, see Scheme 1 for numbering) δ_H: 1.13 (d, $^3J_{HH}$ = 6.8 Hz, 6H, H^{o-2}), 3.70 (sep, $^3J_{HH}$ = 6.8 Hz, 1H, H^{o-1}), 6.81 (m, 1H, H^6), 7.07 (m, 1H, H^5), 7.25–7.28 (m, 4H, H^{8*}), 7.31–7.35 (m, 8H, H^3, H^4, H^{9*} and H^{10*}). Although ligand **2** is a known compound, its synthesis has not been described earlier [30].

*2.1.3. (2-Methylnaphthyl)diphenylphosphane (**3**)*

With the procedure described for (2-cyclohexylphenyl)diphenylphosphane, reactions of 1-bromo-2-methylnaphthalene (4.4 g, 3.1 ml, 20.0 mmol), *n*-butyllithium (8.0 ml, 20.0 mmol) and chlorodiphenylphosphane (4.4 g, 3.6 ml, 20.0 mmol) afforded a crude brown oily product. The oily product was recrystallized several times from ethanol. The yield of the resulting white pure product was 1.6 g, 4.8 mmol, 24%. Exact mass (Micromass LCT, ESI+): 327.1293 $(M + H)^+$ (calcd. for $C_{23}H_{20}P$, 327.1303). ^{1}H-NMR (400 MHz, $CDCl_3$, see Scheme 1 for numbering) δ_H: 2.54 (s, 3H, H^{o-1}), 7.20–7.28 (m, 7H, H^7, H^{9*}, H^{10*}), 7.33–7.40 (m, 6H, H^3, H^6, H^{8*}), 7.79 (d, $^3J_{HH}$ = 8.0 Hz, 1H, H^5), 7.86 (d, $^3J_{HH}$ = 8.4 Hz, 1H, H^4), 8.34 (dd, $^3J_{HH}$ = 8.6 Hz, $^4J_{HP}$ = 4.0 Hz, 1H, H^8).

*2.1.4. (2,5-Dimethylphenyl)diphenylphosphane (**4**)*

This compound was prepared similarly to (2-cyclohexylphenyl)diphenyl phosphane but with chlorodiphenylphosphane replaced by dichloro(2,5-dimethylphenyl)phosphane. Dichloro(2,5-dimethylphenyl)phosphane was synthesized by Friedel–Crafts reaction of phosphorus trichloride with *p*-xylene in the presence of aluminum chloride as catalyst [31]. Reactions of bromobenzene (4.7 g, 3.2 ml, 30.0 mmol), *n*-butyllithium (12.0 ml, 30.0 mmol) and dichloro(2,5-dimethylphenyl)phosphane (3.1 g, 15.0 mmol) afforded a solid light yellow product. The solid product was recrystallized from ethanol. The yield of the resulting white pure product was 4.0 g, 13.8 mmol, 92%. Exact mass (Micromass LCT, ESI+): 291.1325 $(M + H)^+$ (calcd. for $C_{20}H_{20}P$, 291.1303). ^{1}H-NMR (400 MHz, $CDCl_3$, see Scheme 1 for numbering) δ_H: 2.16 (s, 3H, H^{m-1}), 2.34 (s, 3H, H^{o-1}), 6.57 (d, $^3J_{HP}$ = 4.8 Hz, 1H, H^6), 7.06 (dd, $^3J_{HH}$ = 7.7 Hz, $^5J_{HP}$ = 1.3 Hz, 1H, H^4), 7.10 (dd, $^3J_{HH}$ = 7.6 Hz, $^4J_{HP}$ = 4.6 Hz, 1H, H^3), 7.28 (m, 4H, H^{8*}), 7.34 (m, 6H, H^{9*} and H^{10*}). Preparation of **4** has been described in the literature, however, by different method, with lower yield and without interpretation of NMR shifts [32].

*2.1.5. (2-Phenylphenyl)diphenylphosphane (**5**)*

With the procedure described for (2-cyclohexylphenyl)diphenylphosphane, reactions of 2-bromobiphenyl (2.8 g, 2.1 ml, 12.0 mmol), *n*-butyllithium (4.8 ml, 12.0 mmol) and chlorodiphenylphosphane (2.6 g, 12.0 mmol) afforded a crude oily product. The white solid product was obtained by washing the crude product with hexane/ethanol mixture. The product was recrystallized from ethanol. The yield of the white pure product was 2.8 g, 8.3 mmol, 69%. Exact

mass (Micromass LCT, ESI+): 339.1294 $(M + H)^+$ (calcd. for $C_{24}H_{20}P$, 339.1303). ^{1}H-NMR (400 MHz, $CDCl_3$, see Scheme 1 for numbering) δ_H: 7.06 (m, 1H, H^6), 7.16–40 (m, 18H, H^3, H^4, H^5, H^{8*}, H^{9*}, H^{10*}, $H^{o\text{-}2}$, $H^{o\text{-}3}$ and $H^{o\text{-}4}$). Preparation of **5** has been described in the literature, but by a different method, and with lower yield [33].

2.2. Rh(acac)(CO)(PR_3) complexes

(Acetylacetonato)dicarbonylrhodium(I) (50 mg, 0.19 mmol) and the phosphane ligand (0.19 mmol) were dissolved in minimum amount of tetrahydrofuran in separate flasks. The solutions containing equimolar amounts of Rh(acac)$(CO)_2$ and phosphane (PR_3) were combined and stirred at room temperature overnight. After that the solution was evaporated to dryness in vacuum. Spectroscopic data of the compounds in Table 2 are characteristic of Rh(acac)(CO)(PR_3) species. However, attempts to crystallize the compound for further studies were not successful.

2.3. Computational details

We used Gaussian 94 [34] and Sybyl 6.03 [35] programs in modeling. No special geometry around the phosphorus was used in ligand modeling. Initial guesses of the geometries of Rh(acac)(CO)(PR_3) species were based on the solid state structure of Rh(acac)$(CO)_2$ [36].

Ligand: Structures were optimized on the HF level of theory using the 3-21G* basis set. Optimization was carried out only to release the excess strain and thus no conformational analysis was performed. For the cone angle measurements, the metal(dummy atom)–phosphorus distance 2.28 Å and van der Waals' radius of hydrogen 1.2 Å were used.

Complexes: Hartree–Fock and two density functional methods, namely B3LYP and B3PW91, were used for the geometry optimization of complex structures. Calculations of Rh(acac)$(CO)_2$, Rh(CO)Cl(SP) (SP = (2-thiomethylphenyl)diphenylphosphane), and Rh(CO)Cl(NP) (NP = (2-dimethylaminophenyl)diphenylphosphane) were carried out with three different basis sets: 3-21G*, 6-31G* and 6-31+G*. Calculations of Rh(acac)(CO)(PR_3) species were carried out with the combination B3PW91/6-31G*.

2.4. Hydroformylation of propene and 1-hexene

Propene hydroformylation: Experiments were carried out in a 250 ml autoclave (Berghof) equipped with a sampling system and a 230 ml Teflon liner. The experiments were done in semi-batch mode so that synthesis gas pressure was kept constant during the experiment. The rhodium precursor was $Rh(NO_3)_3$ (Fluka). In a typical experiment, the autoclave was charged with the rhodium precursor (0.02 mmol calculated as rhodium), acetone (310 mmol, Merck, >99%), internal standards decane (7 mmol, Fluka, >98%) and hexane (12 mmol, Riedel de Häen, >99%) and the phosphane. The ligand to rhodium ratio was 10:1 on molar basis. The system was flushed with nitrogen and pressurized with propene (2 bar, Aga, 99.8%), heated to the reaction temperature (100 °C) with continuous stirring, and then pressurized to the reaction pressure (10 bar) with a 1:1 molar ratio of H_2 and CO (MG, 99.997%). At least nine samples were taken for analysis in each experiment: one of the fresh reaction, one immediately after pressurizing with H_2 and CO, which was considered as the starting point of the reaction, six during the experiment and one after the reaction.

1-Hexene hydroformylation: Experiments were conducted in a 100 ml autoclave (Berghof) with 60 ml Teflon liner. The experiments were done in batch mode with rhodium precursor Rh(acac)$(CO)_2$. The reactor was charged under a nitrogen purge with substrate, rhodium catalyst, ligand (L/Rh 50) and internal standard cyclohexane. The autoclave was then sealed and pressurized with a 1:1 mixture of H_2 and CO (MG, 99.997%) to 25 bar and heated to 80 °C. After 4 h, the autoclave was cooled and brought to normal atmospheric pressure.

The procedure was the same for the two alkenes: a disposable inner Teflon liner was used to avoid the accumulation of rhodium on the reactor walls. Furthermore, the purity of the system was checked with blank runs before each experiment. The products were analyzed with a Hewlett-Packard 5890 GC equipped with a capillary column (HP-1, 1.0 μm × 0.32 mm × 60 m) and a flame-ionization detector. Products were quantified by the internal standard method. In addition, the aldehydes were identified by GC–MS analysis. Conversion, selectivity and *i*/*n* ratio were calculated on molar basis. Conversion was calculated with respect to propene (1-hexene) and selectivity with respect to

aldehydes. The *i*/*n* ratio of the aldehydes was defined as the amount of branched product divided by the amount of linear product. Hydrogenation was not detected in any of the experiments.

3. Results and discussion

3.1. Synthesis of free ligands

This study is a continuation of our previous study on ligands *o*-MeP, *o*-EtP and 2,4,5-MeP. The present ligands, **1**–**5**, likewise represent modifications of the *o*-position of the aromatic, PPh_3-like, structure, are bulkier than those of our previous study [4,29]. The ligands were prepared by a modified literature method from *o*-substituted brominated aromatics by lithiation with *n*-butyllithium and further reaction with arylchlorophosphanes [19]. The yields were reasonably good (69–92%) except for **2** and **3**, which required several washing and recrystallization steps and appeared in lower yield (23 and 24%).

3.2. Characterization of free ligands

The structural characterization of the ligands was done by NMR methods. In $^{13}C\{^1H\}$-NMR spectra, the chemical shifts for phenyl carbons (Scheme 1, marked 7*, 8*, 9*, 10*), *o*-substituted aromatic ring carbons 1, 2 and 6, substituent carbons *o*-1 and *m*-1, and naphthyl ring carbons 1 and 2 could be assigned for all ligand structures (Table 1). The unconfirmed ^1H-NMR shifts were assigned on the basis of the reliable information from two-dimensional NMR spectra: (H, C)-correlated HSQC, (H, H)-correlated COSY-90 and long-range (C, H)-correlated COLOC. Even then, however, the multiplicity could not be identified for all of the aromatic spin systems and cyclohexyl substituent because of signal overlap. Two-dimensional spectra were necessary in the assignment of ^{13}C chemical shifts of the carbons 3–5 (Scheme 1) and also the carbons of the naphthyl ring.

3.3. Ab initio calculations of free ligands

The optimization procedure led to a geometry where with just one exception, the *o*-substituents were located outside the cone. Owing to the much lower steric repulsion, in the case of *o*-MeP and **3**, the substituent was placed inside the cone. The calculated cone angles of the free ligands are given in Scheme 1. As substantial effect of the size of the ligand on the cone angle was observed by modifying the *o*-position. Compared with PPh_3 (149°) the cone angle increased from 184° for **1** to 191° for **5**. An even larger increase from *o*-MeP (151°) to **3** (223°) occurred when one *o*-methyl substituted benzene ring was replaced with an *o*-methyl substituted naphthyl ring.

3.4. Syntheses of complexes

Reaction between equimolar amounts of Rh(acac)$(CO)_2$ and phosphanes (PR_3) afforded rhodium complexes with the general formula Rh(acac)(CO)(PR_3). Spectroscopic ($^{31}P\{^1H\}$-NMR, FT-IR) characterizations of the Rh(I) complexes are summarized in Table 2.

3.5. Ab initio calculations of complexes

Molecular modeling methods were also applied to the structures of complexes. The stereoelectronic nature of the coordinated ligands was expected to provide valuable information for the structure activity search, especially because the crystallization of the Rh(acac)(CO)(PR_3) species failed.

The Rh(acac)$(CO)_2$ derivatives were chosen as model compounds for the search for the appropriate method and level of calculation. As in the case of free ligand optimization, Hartree–Fock method was applied to the complexes. Two density functional methods, B3LYP and B3PW91, were studied as well. Results are shown in Table 3. As expected, the inadequacy of the HF method to handle electron correlation was evident. In particular, HF failed to predict the inter-atomic distances by overestimating the Rh–C and Rh–O distances. Two density functional methods gave better agreement with the solid-state structures. The agreement got better moving from 3-21G* to 6-31G*, but failed to improve with the use of 6-31+G*. This was considered to be related to the relativistic effects found on second-row transition metals. The evaluation of the two density functional methods was, therefore, continued with 6-31G*. To take into account the effect of the coordinated phosphane ligand, two additional complexes, Rh(CO)Cl(SP)

Table 3
Standard deviation in bond distances and angles between the solid-state structure and gas-phase structure

Basis set	HF	B3LYP	B3PW91
$Rh(acac)(CO)_2$			
3-21G*	0.040/1.991	0.022/0.874	0.019/0.803
6-31G*	0.058/1.862	0.021/0.831	0.015/0.724
6-31+G*		0.023/0.841	0.017/0.706
RhCOCl(SP)[a]			
6-31G*		0.021/1.52	0.012/1.36
RhCOCl(NP)[b]			
6-31G*		0.013/1.60	0.011/1.58

[a] SP = (2-thiomethylphenyl)diphenylphosphane.
[b] NP = (2-dimethylaminophenyl)diphenylphosphane.

(SP = (2-thiomethylphenyl)diphenylphosphane) and Rh(CO)Cl(NP) (NP = (2-dimethylaminophenyl)diphenylphosphane), were selected for study. Both DFT methods gave reasonable accuracy, with B3PW91 method taking a slight edge over B3PW91 accompanied with the 6-31G* basis set. Thus, B3PW91/6-31G* was the choice for the computational treatment for $Rh(acac)(CO)(PR_3)$ species.

Because of the convergence failures with the optimization procedure, only three complexes were successfully optimized: Rh(acac)(CO)(**3**), Rh(acac)(CO)-(**5**) and Rh(acac)(CO)(*o*-MeP) (Scheme 2). The third was considered to be an adequate model for Rh(acac)(CO)(**4**) and Rh(acac)(CO)(**2**) as well.

Cone angle measurements of the coordinated ligands differed significantly from those of the free ligand (see Scheme 2). This is most clearly seen with ligand **3**. In free ligand state it is energetically favorable to bend the naphthyl ring away from the rest of the structure, leaving the methyl group inside the cone. In coordinated state the naphthyl ring rotates as far as possible from the metal center, leaving the methyl group directed towards the rhodium. Such behavior is a good example of the situation where the free ligand structure does not give even a qualitative picture of the coordinated state and there is a huge difference in the cone angle values for coordinate and free state (159 and 223°, respectively). Correspondingly the cone angle values for the free and bound ligand **5** were 191° versus 177°.

The methyl group is also directed towards the metal center in the case of coordinated *o*-MeP ligand.

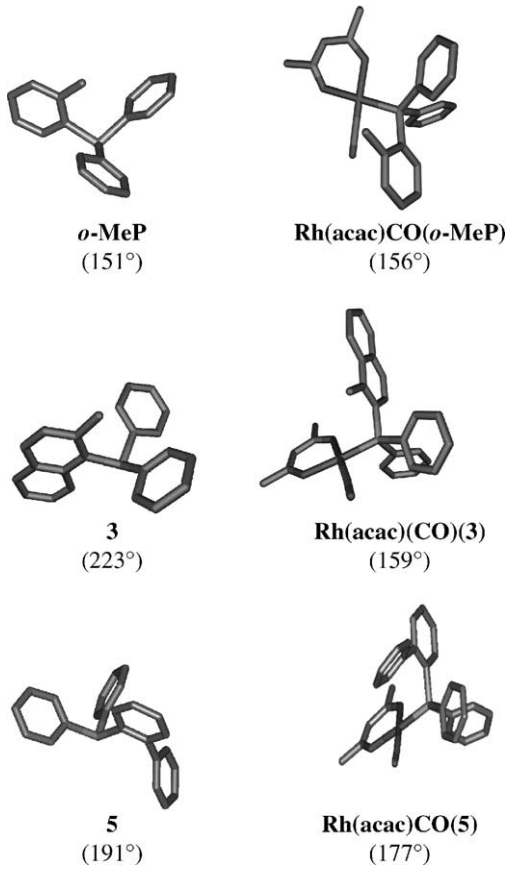

Scheme 2. Gas-phase structures of free and coordinated ligands and their calculated cone angles.

Further evidence of this was provided by X-ray crystallography of *trans*-$Rh(CO)Cl(o\text{-MeP})_2$ complex [29]. It is reasonable to believe that a similar situation is prevails for **2** and **4**. Similarly the coordinated **5** must model the coordinated ligand **1** adequately enough.

3.6. Hydroformylation of propene

Results from the hydroformylation of propene are displayed in Table 4. The disadvantages of the unmodified rhodium catalyst are that the initial activity and conversion of the propenes hydroformylation reaction are very low, even though the regioselectivity to produce isobutanal was 57% under the conditions employed. The widely used ligand PPh_3 was, therefore, chosen as a good reference for the prepared ligands.

Table 4
Results for hydroformylation of propene by rhodium catalysts with *o*-substituted aromatic phosphane ligands

Ligand	θ (°)	δ_P (ppm)	X (%)	Initial rate (mol/(mol$_{Rh}$ s))	$S_{isobutanal}$ (%)	i/n
1	184	−13.6	67	26	46.0	0.85
2	187	−13.8	63	24	47.0	0.89
3	223	−16.5	46	17	45.0	0.82
4	159	−9.5	70	23	43.0	0.75
5	191	−11.9	45	11	48.5	0.94
o-MeP	151	−10.7	81	35	44.0	0.79
2,4,5-MeP	159	−11.8	50	20	45.0	0.82
PPh_3	149	−3.3	97	45	36.0	0.56
No ligand	–	–	10 (3 h)	–	57.0	1.3

Reaction conditions: 10 bar ($CO/H_2 = 1$), $T = 100\,°C$, X = conversion = 2 h, propene/Rh = 512, L/Rh = 10. Initial rate for aldehyde formation. *o*-MeP = (2-methylphenyl)diphenylphosphane and 2,4,5-MeP = (2,4,5-trimethylphenyl)diphenylphosphane.

Our *o*-substituted ligands gave considerably higher *i*/*n* ratios than triphenylphosphane. Relative to PPh_3, the selectivity to isobutanal increased from 43 to 48.5% for all ligands studied, and the initial activity decreased from 11 to 35 mol/(mol$_{Rh}$ s). Still, the *n*-butanal continued to be the main product.

The regioselectivity of the hydroformylation reaction is determined by the stereoelectronic factors of the catalytically active complex. According to previous studies, the more basic the phosphane the less active it is and the higher the *i*/*n* ratio [12,37–39]. Carbonyl stretching frequencies of metal complexes are used as a measure of the basicity of phosphanes [6]. In our work, however, the only narrow range of the carbonyl IR stretching frequencies for Rh(acac)(CO)(PR_3) complexes (Table 2) did not reveal any clear correlation with the propene hydroformylation results. Even though the regioselectivities of the rhodium catalysts with studied ligands were similar, there could be seen slight increase in *i*/*n* ratios as the cone angle of *o*-substituted phenylphosphane was between 184 and 191° compared to *o*-methyl-substituted phenylphosphanes (151–159°). The cone angles seems to give also a rough ordering with respect to conversion. The bulkier the phosphane, the lower the conversion.

The electronegativity of substituents on phosphorus and the angles between them are the two most important variables determining $^{31}P\{^1H\}$-NMR chemical shift, and hence the shift characterize both the electronic nature and steric nature of the phosphorus atom [5]. Evidently, the ligands are electronically very similar and differences in $^{31}P\{^1H\}$-NMR chemical shifts are attributable mostly from large range of cone angles caused by steric crowding of the *o*-substituted phenylphosphanes. The cone angles increase with downfield $^{31}P\{^1H\}$-NMR chemical shift. Ligands with $^{31}P\{^1H\}$-NMR shift between −9.5 and −11.8 ppm are *o*-methyl-substituted phenylphosphanes (15–159°) and the bulky *o*-cyclohexyl- or *o*-isopropyl-substituent containing phenylphosphanes (184–187°) have $^{31}P\{^1H\}$-NMR shift around −13.6 to −13.8 ppm. Comparison of the structurally similar *o*-alkyl-substituted ligands (**1**–**3** and *o*-MeP) with PPh_3 shows previously reported trend between the $^{31}P\{^1H\}$-NMR shift and the selectivity to isobutanal and the initial activity [4]. The selectivities increase and the initial activities decrease as the $^{31}P\{^1H\}$-NMR shift of the free ligand decreases.

The decrease in the initial activity is more marked than the increase in the selectivity. Relative to PPh_3, the most notable difference in the initial activity is observed for the phenyl substituted ligand **5** and the smallest for *o*-MeP. Even rigid naphthylphosphane **3** had less suppressing effect on the initial activity than did **5**. This may be a reflection of the smaller cone angle of the coordinated ligand **3** than of the coordinated **5**. Both the ligands containing *m*- and *p*-methyl substituents (**4** and 2,4,5-MeP) and the ligands containing bulkier *o*-alkyl-substituent (**1** and **2**) decreased the initial activity more than did *o*-MeP, even though the selectivity to form isobutanal was more or less the same with the five ligands. On the average, *o*-MeP would seem to represent an optimum between activity and selectivity.

Table 5
Results for hydroformylation of 1-hexene by rhodium catalysts with *o*-substituted aromatic phosphane ligands

Ligand	θ (°)	δ_P (ppm)	X (%)	$S_{2\text{-hex}}$ (%)	$S_{3\text{-hex}}$ (%)	$S_{2\text{-mh}}$ (%)	$S_{1\text{-hep}}$ (%)	i/n
1	184	−13.6	90	2	4	30	63	0.48
2	187	−13.8	59	0	5	32	64	0.50
3	223	−16.5	99	4	10	26	60	0.43
4[a]	159	−9.5	2	0	0	0	100	–
5	191	−11.9	99	3	9	29	59	0.49
PPh_3	149	−3.3	82	2	3	24	71	0.34

Reaction conditions: 25 bar (CO/H_2 = 1), T = 80 °C, X = conversion = 4 h, 1-hexene 15.5 mmol, toluene 10 ml, $Rh(acac)(CO)_2$ 1.9×10^{-2} mmol, L/Rh = 50. $S_{2\text{-hex}}$ = total amount of 2-hexene; $S_{3\text{-hex}}$ = total amount of 3-hexene; $S_{2\text{-mh}}$ = selectivity to 2-methylhexanal; $S_{1\text{-hep}}$ = selectivity to 1-heptanal.

[a] At 20 bar and 100 °C, and 1-hexene:Rh = 10,000: X = 98%, $S_{2\text{-hex}}$ = 61%, $S_{3\text{-hex}}$ = 18%, $S_{2\text{-ep}}$ = 2%, $S_{2\text{-mh}}$ = 8%, $S_{1\text{-hep}}$ = 11% and i/n = 0.91. $S_{2\text{-ep}}$ = selectivity to 2-ethylpentanal.

3.7. Hydroformylation of 1-hexene

Results from the 1-hexene hydroformylation tests are compiled in Table 5. All the catalyst systems afforded relatively high chemoselectivity to aldehydes, with 1-heptanal and 2-methylhexanal the major products. Only small amounts of 2- and 3-hexene were formed, and thus 2-ethylpentanal was not formed at all. The low conversion with the *o*–*m*-methyl-substituted ligand **4** (2%) is in accordance with our earlier results for 2,4,5-MeP, which likewise did not form an active catalyst at 80 °C, but restored the activity when the temperature was raised to 100 °C (Table 5) [29].

The modified ligands gave considerably higher *i*/*n* ratios than triphenylphosphane. The effect was the same as with propene but less pronounced. Likewise, there were similarities between the two alkenes in the branched aldehyde formation. However, the effect of the modified ligands on branching was less in the case of 1-hexene than propene. Relative to PPh_3, the selectivity of the modified catalyst to 2-methylhexanal increased from 2 to 8%. The catalyst systems containing **1**, **2** and **5** and gave the highest *i*/*n* ratios.

Despite of the different experimental setups, hydroformylation of the two alkenes with the ligand-modified rhodium catalysts showed similar trends, which were also in agreement with findings in our earlier studies with *o*-MeP, *o*-EtP and 2,4,5-MeP ligands [4]. Relative to triphenylphosphane, steric bulk due to the *o*-modification affected the selectivity to the branched aldehyde formation positively. Evidently, without any substituents, PPh_3 (149°) is capable of competing in binding with (against) CO, and the formed $HRh(CO)_2(PPh_3)_2$ species gives rise to lower *i*/*n* ratio. In contrast to this, the sterically hindered *o*-modified phosphanes favors the formation of $HRh(CO)_3(PR_3)$ species. As a result, CO dissociation is more likely to occur, and the formed $16e^-$ complexes with the large space available are favorable for producing branched alkylrhodium species and enhanced *i*/*n* ratios [8–10,12]. However, sterically demanding *o*-alkyl-substituted phenylphosphanes have lower π-acceptor ability than *o*-alkyl-substituted phenylphosphites even then they both have large cone angle [8]. Due to that the catalytically active rhodium center become less electrophilic and probably hence, the reactivity will decrease.

4. Conclusion

We have shown that, in the rhodium-catalyzed hydroformylation, a wider group of *o*-alkyl-substituted aromatic phosphane ligands enhance the selectivity to branched aldehydes. The effect of the modified ligands on branching is less pronounced in the case of 1-hexene compared to propene. The steric stress of *o*-alkyl-substituent has significant influence both on the formation of active rhodium species and catalytic reaction. The regioselectivity to isobutanal increase and the initial activity decrease as the cone angle increase with downfield $^{31}P\{^1H\}$-NMR chemical shift of closely related free ligand. Most probably the formation of $HRh(CO)_3(PR_3)$ species are due to the increased *i*/*n* ratios. However, the simultaneous

optimization of reactivity and selectivity constitutes a major challenge for the future.

Acknowledgements

We gratefully acknowledge the financial support from Neste Oxo AB and the National Technology Agency of Finland (Tekes). We wish to thank Ms. Päivi Joensuu and Ms. Sari Ek for the mass spectra, Ms. Merja Harteva for performing part of the propene hydroformylation tests and Ms. Liisa Saharinen for assistance in the 1-hexene hydroformylation tests and preparation of rhodium complexes.

References

[1] B. Breit, W. Seiche, Synthesis 1 (2001) 1.
[2] A.M. Trzeciak, J.J. Ziółkowski, Coord. Chem. Rev. 190–192 (1999) 883.
[3] M. Beller, B. Cornils, C.D. Frohning, C.W. Kohlpaintner, J. Mol. Catal. A: Chem. 104 (1995) 17.
[4] H.K. Reinius, P. Suomalainen, H. Riihimäki, E. Karvinen, J. Pursiainen, A.O.I. Krause, J. Catal. 199 (2001) 302.
[5] C.A. Tolman, Chem. Rev. 77 (1977) 313.
[6] C.A. Tolman, J. Am. Chem. Soc. 92 (1970) 2953.
[7] C.A. Tolman, J. Am. Chem. Soc. 92 (1970) 2956.
[8] P.W.N.M. van Leeuwen, C.F. Roobeek, J. Organomet. Chem. 258 (1983) 343.
[9] T. Jongsma, G. Challa, P.W.N.M. van Leeuwen, J. Organomet. Chem. 421 (1991) 121.
[10] S.N. Poelsma, P.M. Maitlis, J. Organomet. Chem. 451 (1993) C15.
[11] A. van Rooy, E.N. Orij, P.C.J. Kamer, P.W.N.M. van Leeuwen, Organometallics 14 (1995) 34.
[12] B. Cornils, W.A. Herrmann, Applied Homogeneous Catalysis with Organometallic Compounds, vol. 1, VCH, Weinheim, 1996, Chapter 2, pp. 58–59.
[13] C.J. Elsevier, B. Kowall, H. Kragten, Inorg. Chem. 34 (1995) 4836.
[14] S. Song, E.C. Alyea, Can. J. Chem. 74 (1996) 2304.
[15] T.L. Brown, K.J. Lee, Coord. Chem. Rev. 128 (1993) 89.
[16] J.M. Smith, B.C. Taverner, N.J. Coville, J. Organomet. Chem. 530 (1997) 131.
[17] D. White, N.J. Colville, Adv. Organomet. Chem. 36 (1994) 99.
[18] J. Bruckmann, C. Krüger, F. Lutz, Z. Naturforsch. 50b (1995) 351.
[19] G. Dyer, D.W. Meek, J. Am. Chem. Soc. 89 (1967) 3983.
[20] E.G. Hope, T. Kemmitt, W. Levason, J. Chem. Soc., Perkin Trans. II (1987) 487.
[21] L. Horner, G. Simons, Phosphorus Sulfur 14 (1983) 189.
[22] L. Horner, G. Simons, Phosphorus Sulfur 15 (1983) 165.
[23] R.H. Laitinen, V. Heikkinen, M. Haukka, A.M.P. Koskinen, J. Pursiainen, J. Organomet. Chem. 598 (2000) 235.
[24] P. Suomalainen, S. Jääskeläinen, M. Haukka, R.H. Laitinen, J. Pursiainen, T.A. Pakkanen, Eur. J. Inorg. Chem. (12) (2000) 2607.
[25] H.K. Reinius, R.H. Laitinen, A.O.I. Krause, J.T. Pursiainen, Stud. Surf. Sci. Catal. 130 (2000) 551.
[26] P. Suomalainen, H.K. Reinius, H. Riihimäki, R.H. Laitinen, S. Jääskeläinen, M. Haukka, J.T. Pursiainen, T.A. Pakkanen, A.O.I. Krause, J. Mol. Catal. A: Chem. 169 (2001) 67.
[27] C.B. Ziegler, R.F. Heck, J. Org. Chem. 43 (1978) 2941.
[28] F. Ancilotti, M. Lamiand, M. Marchionna, J. Mol. Catal. 63 (1990) 15.
[29] P. Suomalainen, H. Riihimäki, S. Jääskeläinen, M. Haukka, J.T. Pursiainen, T.A. Pakkanen, Catal. Lett. 77 (2001) 125.
[30] H.J. Jakobsen, T. Liptaj, T. Bundgaard, S. Sørensen, J. Magn. Reson. 26 (1977) 71.
[31] B. Buchner, L.B. Lockhart, J. Am. Chem. Soc. 73 (1951) 755.
[32] H. Schindlbauer, Monatsh. Chem. 96 (1965) 2051.
[33] F. Mitterhofer, H. Schindlbauer, Monatsh. Chem. 98 (1967) 206.
[34] M.J. Frish, G.A. Petersson, J.A. Montgomery, K. Raghavachari, M.A. Al-Lahman, V.G. Zakrzewski, J.V. Ortiz, J.B. Foresman, J. Ciolowski, B.B. Stefanov, A. Nanayakkara, M. Challacombe, C.Y. Peng, P.Y. Ayala, W. Chen, M.W. Wong, J.L. Andres, E.S. Replogle, R. Gomperts, R.L. Martin, D.J. Fox, J.S. Binkley, D.J. Defrees, J. Baker, J.P. Stewart, M. Head-Gordon, C. Gonzales, J.A. Pople, Gaussian Inc., Pittsburgh, PA, 1995.
[35] Sybyl 6.03, Tripos Associates, 1699 S. Hanley Road, Suite 303, St. Louis, MO 63144, USA.
[36] F. Huq, A.C. Skapski, J. Cryst. Mol. Struct. 4 (1974) 411.
[37] C.A. Streuli, Anal. Chem. 32 (1960) 985.
[38] C.A. Streuli, Anal. Chem. 31 (1959) 1652.
[39] W.R. Moser, C.J. Papile, D.A. Brannon, R.A. Duwell, S.J. Weininger, J. Mol. Catal. 41 (1987) 271.